



ELSEVIER

Contents lists available at ScienceDirect

Comptes Rendus Physique

www.sciencedirect.com



Phononic crystals / Cristaux phononiques

How diffraction limits ultrasonic screening in phononic plate composed of a periodic array of resonant slits



Comment la diffraction limite l'opacité ultrasonore d'une plaque phononique composée d'un réseau périodique de fentes résonantes

Aliyasin Elayouch^{a,*}, Mahmoud Addouche^a, Philippe Lasaygues^b,
Younes Achaoui^b, Morvan Ouisse^a, Abdelkrim Khelif^a

^a Institut FEMTO-ST, Université de Franche-Comté, CNRS, 15B avenue des Montboucons, 25030 Besançon cedex, France

^b Laboratoire de mécanique et d'acoustique, UPR CNRS 7051, 31, chemin Joseph-Aiguier, 13402 Marseille cedex 20, France

ARTICLE INFO

Article history:

Available online 2 March 2016

Keywords:

Fabry–Perot acoustic resonator
Acoustic screening
Diffraction
Acoustic metamaterials

Mots-clés :

Résonateur acoustique de Fabry–Perot
Opacité acoustique
Diffraction
Matériaux acoustiques

ABSTRACT

We explore experimentally the role played by diffraction in the phenomenon of acoustic shielding provided by a plate that is periodically perforated with subwavelength slits and immersed in water. We carried out ultrasonic transmission measurements for all directions of propagation in order to check the omnidirectionality of acoustic shielding. While a single slit acts as a Fabry–Perot resonator in the frequency range of interest, the coupling between adjacent slits provides an attenuation frequency band centered around the resonant frequency that is mostly independent of the angle of incidence. Beyond the incident angle of 45 degrees, however, we observe the appearance of scattered radiation that limits the attenuation of ultrasound. This spurious scattering is shown to arise from diffraction by the grating of slits.

© 2016 Académie des sciences. Published by Elsevier Masson SAS. This is an open access article under the CC BY-NC-ND license (<http://creativecommons.org/licenses/by-nc-nd/4.0/>).

R É S U M É

Nous étudions expérimentalement le rôle joué par la diffraction dans le phénomène d'isolation acoustique que présente une plaque phononique perforée périodiquement par des fentes sub-longueur d'onde et plongée dans l'eau. Nous avons effectué des mesures de transmission dans le domaine ultrasonore pour toutes les directions de propagation dans le but de vérifier l'omnidirectionnalité de l'isolation acoustique. Alors qu'une fente se comporte comme un résonateur de Fabry–Pérot dans le domaine de fréquence considéré, le couplage des fentes voisines produit une bande fréquentielle d'atténuation centrée sur la fréquence de résonance et qui est quasiment indépendante de l'angle d'incidence. Au-delà d'un angle d'incidence de 45 degrés, cependant, nous observons l'apparition

* Corresponding author.

E-mail address: aliyasin.elayouch@femto-st.fr (A. Elayouch).

d'un rayonnement diffracté qui limite l'atténuation ultrasonore. Nous montrons que ce rayonnement indésirable provient de la diffraction associée au réseau de fentes.

© 2016 Académie des sciences. Published by Elsevier Masson SAS. This is an open access article under the CC BY-NC-ND license (<http://creativecommons.org/licenses/by-nc-nd/4.0/>).

1. Introduction

The understanding of wave phenomena has come to a turning point with the arrival of new artificial structures such as phononic crystals and acoustic metamaterials. Their counter-intuitive behavior never ceases to surprise and permits to overcome many challenges in the acoustic domain: one of these is the omnidirectionality of wave attenuation. In this regard, phononic crystals have been demonstrated to exhibit complete band gaps, or frequency ranges where no wave can be transmitted, whatever the direction of propagation [1,2]. Furthermore, resonance-based mechanisms can be efficiently used to control the propagation of acoustic waves. In 2000, the group of P. Sheng opened the way with the introduction of locally-resonant sonic materials that exhibit phononic bandgaps at frequencies that are much lower than those introduced by Bragg scattering in phononic crystals. From this starting point, other structures having a periodic distribution of embedded resonators, generally in the form of inclusions, have emerged. This is the case of structures with inclusions in the form of masses attached to a membrane [3–5], of arrays of pillars on a surface [6–8], or of subwavelength apertures in a plate [9–15]. As a result, the transmission of acoustic waves through a periodically perforated plate has been the subject of a great deal of attention [13,14]. By coupling resonators together, it has been shown that an acoustic screening effect can occur [16–21]. This is in particular the case of structures that are based on the coupling between Fabry–Perot resonators forming an array or grating [22]. Under the conditions of finite impedance ratio between the fluid and the solid, the transmission of an acoustic wave through a periodically perforated plate shows a series of resonances and antiresonances that permit to create, at normal incidence, an acoustic blocking effect, thus breaking the conventional mass-density law for walls. The mass-density law states that the amplitude transmittance for a solid panel in the air is proportional to the inverse of the product ρt , where ρ and t are the density and the thickness of the solid panel, respectively [23]. Although the idea of using periodically perforated plates with subwavelength apertures can be applied to prohibit propagation over a rather broadband frequency range, using resonant cavities for waves coming from different directions of incidence may still limit the operating angular frequency bandwidth.

In this paper, we theoretically and experimentally investigate the effect of diffraction on acoustic opacity when ultrasonic waves impinge the phononic plate for different angles of incidence. Indeed, in addition to being resonators, apertures when forming a periodic array also act as a diffraction grating [24,25]. Ultrasonic measurements were carried out and compared to a finite element model (FEM) implemented with Comsol Multiphysics. The experimental results show an attenuation bandwidth that is maintained up to 45° incidence, but that is closed by diffraction. Simple analytical calculations based on the grating law confirm this explanation.

2. Methods

The considered phononic plate is constituted of a $180 \times 165 \text{ mm}^2$ aluminum plate, perforated with a periodic array of slits. The plate thickness is $t = 5 \text{ mm}$, and there are 33 slits separated by a pitch, or lattice constant, $a = t = 5 \text{ mm}$. The slits are $d = 0.17a = 0.85 \text{ mm}$ wide and 150 mm tall. Ultrasonic experiments were conducted in a water tank at frequencies of a few hundreds of kilohertz. In order to cover a wide frequency range, chirped ultrasonic pulses were generated by a 25-mm-diameter immersion transducer. We used an Imasonic transducer as the transmitter and a Precision Acoustics hydrophone as the receiver. The angles of incidence and of transmission are defined with respect to an axis oriented normally to the plate and passing by the center of the slit array. Both the transducer and the hydrophone can be rotated in the XY plane, as presented schematically in Fig. 1a.

In what follows, we shall compare the transmission of an ultrasonic pulse, with a center frequency of 200 kHz, through the phononic plate for three angles of incidence: at normal incidence $\theta_i = 0^\circ$, at $\theta_i = 30^\circ$, and at $\theta_i = 45^\circ$. Thus, for each incident position of the transducer, the hydrophone measures the complete temporal signal for each rotation angle it is given, from $\theta_{tr} = -60^\circ$ to $+60^\circ$ with a step of 4° . For each measurement configuration, the discrete Fourier transform of an average of 31 temporal measurements is computed in order to estimate a transmission spectrum. Then, the different spectra are combined to present the transmission information as a function of frequency and receiving angle θ_{tr} . In Fig. 2, the radial axis measures frequencies, and the spectral transmission modulus is represented by using a colorbar. In the following, the directional transmission spectrum for a homogeneous plate will be compared to various spectra obtained with the phononic plate at different angles of incidence.

3. Experimental results and discussion

In this section, we present the experimental results corresponding to the setup presented above, by distinguishing the cases of normal and oblique incidence. In the normal incidence case, $\theta_i = 0^\circ$, Fig. 2 shows a comparison between transmis-

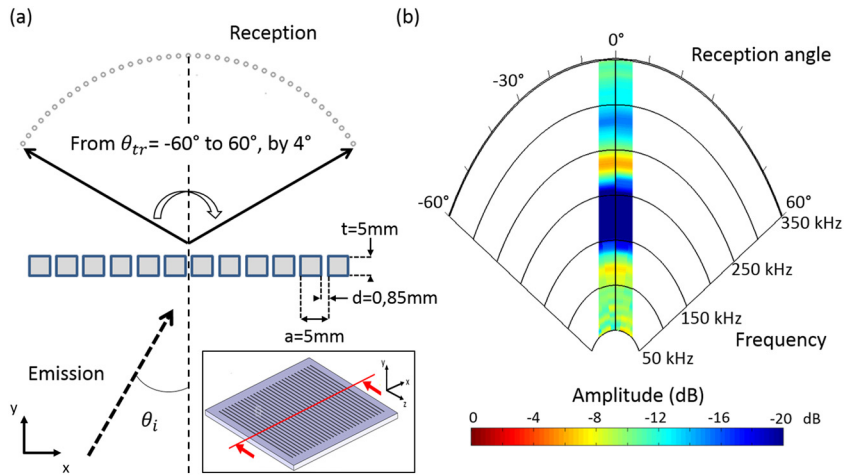


Fig. 1. (a) Schematic of the experimental set-up used for the directional characterization of the phononic plate. The dotted arrows represent the incident direction, making angle θ_i with respect to the normal to the plate. Transmission angles are also defined with respect to the same axis. (b) Experimental directional spectrum obtained for normal incidence ($\theta_i = 0^\circ$) and normal transmission ($\theta_{tr} = 0^\circ$).

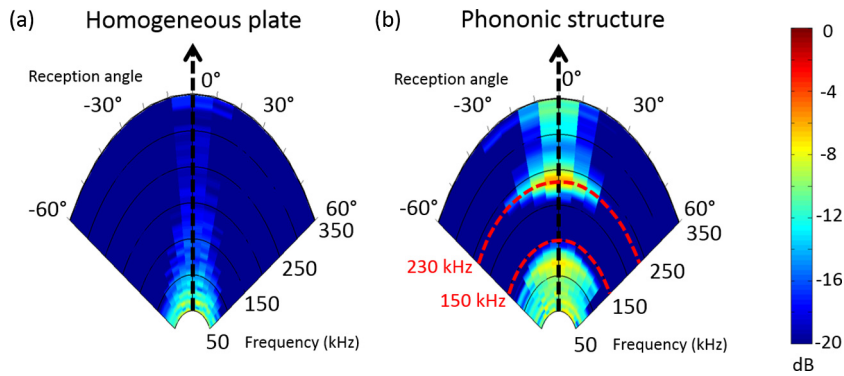


Fig. 2. Angular spectrograms obtained experimentally for normal incidence, for (a) a homogeneous aluminum plate and (b) the phononic plate.

sion spectra obtained with a homogeneous aluminum plate and with the phononic plate. We observe that the direction of propagation of the incident wave is not significantly modified in both cases, since we detect a signal transmitted around the receiving angle $\theta_{tr} = 0^\circ$. Hence, there is no noticeable scattering or diffraction in the case of normal incidence. The difference between the two systems is mainly seen in the attenuation spectrum that follows the classical mass density law for the homogeneous plate, whereas the phononic plate produces an attenuation range extending from around 150 kHz to 200 kHz. In order to confirm these observations, we compare in Fig. 3 the transmission spectra for the homogeneous and the phononic plate as extracted from these measurements in the direction of normal transmission. For the phononic plate, we further compare with the transmission computed by FEM. In the numerical study, we obviously tried to use the same geometrical parameters as those of the experiment. Due to the one-dimensional periodicity of the phononic plate, we carried out the simulation on a unit-cell by applying periodic boundary conditions. Specifically, we assume a time harmonic dependence of the form $e^{-i\omega t}$. The plate domain, made of aluminum, is modeled as an elastic medium using Lamé's equations [26]. In the fluid, sound waves are governed by the following equation for the differential pressure p

$$\nabla \cdot (\rho^{-1} \nabla p) + \frac{\omega^2}{\rho c^2} p = 0 \quad (1)$$

where ρ is the mass density of the fluid, c is the sound speed in water, and ω is the angular frequency of the acoustic pressure wave. The harmonic acoustic pressure in water at the surface of the solid acts as a boundary load in the two-dimensional solid, in order to ensure continuity of pressure through the interface. The finite element model calculates the harmonic displacements and stresses in the solid, using frequency response analysis, and then uses the normal acceleration at the solid surface as a boundary condition for the acoustic domain. The considered physical properties are listed in Table 1. It can be observed that the measured shape of transmission spectra agrees well with the simulation result, with the noticeable occurrence of resonances at frequencies 120 kHz and 230 kHz, as apparent in Fig. 3.

We now consider ultrasonic waves that are incident on the phononic plate with an incident angle of 30° . We observe, in the directional transmission spectrum of Fig. 4a, that the attenuation frequency band is roughly maintained. Indeed,

Table 1

Material properties considered for numerical simulations. c_l and c_t are the longitudinal and shear velocities, respectively.

Material	Density (kg/m ³)	c_l (m/s)	c_t (m/s)
Aluminum	2700	6420	3040
Water	1000	1480	–

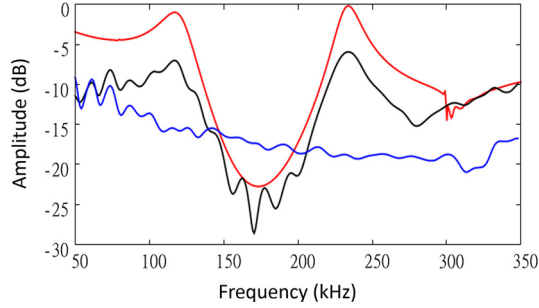


Fig. 3. Measured transmission spectra for the homogeneous aluminum plate (blue line) and the phononic plate (black line), for normal incidence and normal transmission. Numerical simulation with FEM in the case of an infinitely periodic phononic plate is also shown for comparison purposes (red line).

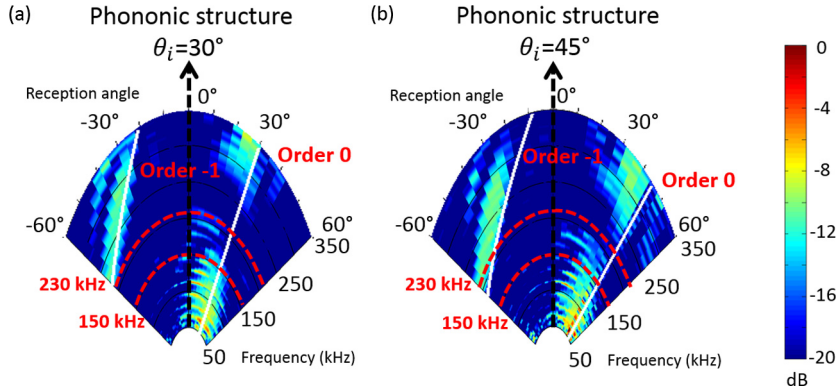


Fig. 4. Angular spectrograms obtained experimentally for the phononic plate, for an angle of incidence of (a) $\theta_i = 30^\circ$ and (b) $\theta_i = 45^\circ$. The white lines show the frequency localization of the orders of diffraction $m = 0$ and -1 obtained analytically from the grating law as $\theta_m = \arcsin(\frac{m\lambda}{a} + \sin\theta_i)$.

the amplitude around the frequency 175 kHz is greatly reduced, as was the case at normal incidence. We also observe the presence of two transmitted plane waves. One of these is such that $\theta_{tr} = \theta_i$ and is thus the expected undiffracted transmitted wave. The second wave we observe, as we argue next, is an order of diffraction of the grating constituted by the periodic array of slits. This order of diffraction is clearly apparent in the directional transmission spectra of Fig. 4, extending from around 200 kHz to 350 kHz. Besides, it can be seen that the transmission angle for this order of diffraction is dispersive, i.e. it depends on frequency.

The experimental results can be simply understood from the grating law applied to the periodic array of slits. Indeed, the phononic plate can be considered as a diffraction grating that obeys the law [27,24]:

$$a(\sin(\theta_m) - \sin(\theta_i)) = m\lambda \tag{2}$$

where m is a relative integer identifying the diffraction order and $\lambda = 2\pi c/\omega$ is the wavelength in water. Thus, for an angle of incidence of 30° , and by considering only the -1 and 0 orders of diffraction, we obtain analytically the curves in Fig. 4. In Fig. 4a, in the angular range $\theta_{tr} = [-60^\circ : +60^\circ]$, we can observe the $m = 0$ order of diffraction for which $\theta_m = \theta_i$ for all frequencies. The $m = -1$ order of diffraction is in contrast dispersive since $\sin(\theta_{tr}) = \sin(\theta_{-1}) = \sin(\theta_i) - \frac{\lambda}{a}$. From the grating law, it can be observed that there is an onset frequency starting from which the order of diffraction becomes propagating. This onset frequency is

$$\omega_m = \frac{2\pi c}{a} \frac{1}{1 - m \sin\theta_i} \tag{3}$$

For $\theta_i = 45^\circ$, the onset frequency for $m = -1$ is about 200 kHz, which is still above the target acoustic shielding frequency range. Correspondingly, we notice in the experimental spectrogram of Fig. 4a that attenuation is maintained around 175 kHz.

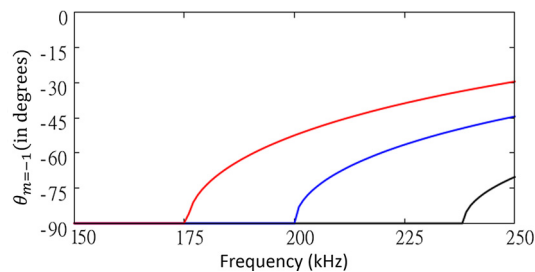


Fig. 5. Frequency dependence of the propagation angle for order of diffraction $m = -1$ for $\theta_i = 15^\circ$ (black line), $\theta_i = 30^\circ$ (blue line), and $\theta_i = 45^\circ$ (red line).

This is not the case for the angle of incidence $\theta_i = 45^\circ$, as can be seen in Fig. 4b. Actually, the $m = -1$ diffraction order becomes propagating around this frequency and the acoustic shielding frequency range is affected. Based on the grating law, we show in Fig. 5 the frequency dependence of the propagation angle for order of diffraction $m = -1$, for different angles of incidence. For $\theta_i = 45^\circ$, diffraction starts at 175 kHz, which is about the center of the attenuation frequency band.

4. Conclusion

In summary, we have demonstrated experimentally that diffraction can strongly limit the omnidirectional character of ultrasonic screening in the case of a phononic plate composed of a periodic array of sub-wavelength resonant slits. We have obtained transmission extinctions up to 20 dB, with a relative bandwidth of 15%, up to an angle of incidence of 45° . Above this value, however, acoustic shielding appears to be degraded. We have shown that this degradation results from the $m = -1$ order of diffraction becoming propagating in the frequency range of interest. Because the onset frequency for a particular order of diffraction is chiefly determined by periodicity at the interface between solid and water, irrespective of the resonant frequency of the slits, it should be possible to design a phononic plate exhibiting omnidirectional acoustic screening. For instance, filling the slits with a different fluid in order to shift down the resonance frequency could provide a solution. Overcoming the diffraction limitation to acoustic screening may enable a much wider range of applications, particularly for underwater acoustics and ultrasonics.

Acknowledgements

Fruitful discussions with Vincent Laude and Sarah Benchabane are gratefully acknowledged. The research leading to these results has received funding from the Région de Franche-Comté and financial support from the Labex ACTION program (Contact No. ANR-11-LABX-0001-01), as well as the support of the French National Research Agency (project ANR-12-JS09-008-COVIA).

References

- [1] M. Sigalas, E.N. Economou, Band structure of elastic waves in two dimensional systems, *Solid State Commun.* 86 (3) (1993) 141–143, [http://dx.doi.org/10.1016/0038-1098\(93\)90888-T](http://dx.doi.org/10.1016/0038-1098(93)90888-T), <http://www.sciencedirect.com/science/article/pii/003810989390888T>, 00517.
- [2] M.S. Kushwaha, P. Halevi, L. Dobrzynski, B. Djafari-Rouhani, Acoustic band structure of periodic elastic composites, *Phys. Rev. Lett.* 71 (13) (1993) 2022–2025, <http://dx.doi.org/10.1103/PhysRevLett.71.2022>, 01364.
- [3] Z. Yang, H.M. Dai, N.H. Chan, G.C. Ma, P. Sheng, Acoustic metamaterial panels for sound attenuation in the 50–1000 Hz regime, *Appl. Phys. Lett.* 96 (4) (2010) 041906, <http://dx.doi.org/10.1063/1.3299007>, <http://scitation.aip.org/content/aip/journal/apl/96/4/10.1063/1.3299007>.
- [4] G. Ma, M. Yang, Z. Yang, P. Sheng, Low-frequency narrow-band acoustic filter with large orifice, *Appl. Phys. Lett.* 103 (1) (2013) 011903, <http://dx.doi.org/10.1063/1.4812974>, http://apl.aip.org/resource/1/applab/v103/i1/p011903_s1.
- [5] J. Mei, G. Ma, M. Yang, Z. Yang, W. Wen, P. Sheng, Dark acoustic metamaterials as super absorbers for low-frequency sound, *Nat. Commun.* 3 (2012) 756, <http://dx.doi.org/10.1038/ncomms1758>.
- [6] A. Khelif, Y. Achaoui, B. Aoubiza, In-plane confinement and waveguiding of surface acoustic waves through line defects in pillars-based phononic crystal, *AIP Adv.* 1 (4) (2011) 041404, <http://dx.doi.org/10.1063/1.3675923>, <http://scitation.aip.org/content/aip/journal/adva/1/4/10.1063/1.3675923>.
- [7] A. Khelif, Y. Achaoui, S. Benchabane, V. Laude, B. Aoubiza, Locally resonant surface acoustic wave band gaps in a two-dimensional phononic crystal of pillars on a surface, *Phys. Rev. B* 81 (21) (2010) 214303, <http://dx.doi.org/10.1103/PhysRevB.81.214303>.
- [8] V. Laude, L. Robert, W. Daniau, A. Khelif, S. Ballandras, Surface acoustic wave trapping in a periodic array of mechanical resonators, *Appl. Phys. Lett.* 89 (8) (2006) 083515, <http://dx.doi.org/10.1063/1.2338523>, <http://scitation.aip.org/content/aip/journal/apl/89/8/10.1063/1.2338523>.
- [9] H. Estrada, P. Candelas, A. Uris, F. Belmar, F. Meseguer, F.J. García de Abajo, Influence of the hole filling fraction on the ultrasonic transmission through plates with subwavelength aperture arrays, *Appl. Phys. Lett.* 93 (1) (2008) 011907, <http://dx.doi.org/10.1063/1.2955825>, http://apl.aip.org/resource/1/applab/v93/i1/p011907_s1.
- [10] X. Wang, Acoustical mechanism for the extraordinary sound transmission through subwavelength apertures, *Appl. Phys. Lett.* 96 (13) (2010) 134104, <http://dx.doi.org/10.1063/1.3378268>, http://apl.aip.org/resource/1/applab/v96/i13/p134104_s1.
- [11] L. Zhou, G.A. Kriegsmann, Complete transmission through a periodically perforated rigid slab, *J. Acoust. Soc. Am.* 121 (6) (2007) 3288–3299, <http://dx.doi.org/10.1121/1.2721878>, <http://link.aip.org/link/?JAS/121/3288/1>.
- [12] Z. He, S. Peng, R. Hao, C. Qiu, M. Ke, J. Mei, Z. Liu, Extraordinary acoustic reflection enhancement by acoustically transparent thin plates, *Appl. Phys. Lett.* 100 (9) (2012) 091904, <http://dx.doi.org/10.1063/1.3691182>, http://apl.aip.org/resource/1/applab/v100/i9/p091904_s1.
- [13] H. Estrada, P. Candelas, A. Uris, F. Belmar, F. Meseguer, F.J. García de Abajo, Sound transmission through perforated plates with subwavelength hole arrays: a rigid-solid model, *Wave Motion* 48 (3) (2011) 235–242, <http://dx.doi.org/10.1016/j.wavemoti.2010.10.008>, <http://www.sciencedirect.com/science/article/pii/S0165212510001022>.

- [14] J. Christensen, L. Martin-Moreno, F.J. Garcia-Vidal, Theory of resonant acoustic transmission through subwavelength apertures, *Phys. Rev. Lett.* 101 (1) (2008) 014301, <http://dx.doi.org/10.1103/PhysRevLett.101.014301>.
- [15] F. Liu, F. Cai, Y. Ding, Z. Liu, Tunable transmission spectra of acoustic waves through double phononic crystal slabs, *Appl. Phys. Lett.* 92 (10) (2008) 103504, <http://dx.doi.org/10.1063/1.2896146>, http://apl.aip.org/resource/1/applab/v92/i10/p103504_s1.
- [16] X. Zhang, Acoustic resonant transmission through acoustic gratings with very narrow slits: multiple-scattering numerical simulations, *Phys. Rev. B* 71 (24) (2005) 241102, <http://dx.doi.org/10.1103/PhysRevB.71.241102>.
- [17] M. Lu, Extraordinary acoustic transmission through a 1d grating with very narrow apertures, *Phys. Rev. Lett.* 99 (2007) 174301, <http://dx.doi.org/10.1103/PhysRevLett.99.174301>.
- [18] F. Liu, M. Ke, A. Zhang, W. Wen, J. Shi, Z. Liu, P. Sheng, Acoustic analog of electromagnetically induced transparency in periodic arrays of square rods, *Phys. Rev. E, Stat. Nonlinear Soft Matter Phys.* 82 (2 Pt 2) (2010) 026601.
- [19] S. Peng, C. Qiu, Z. He, Y. Ye, S. Xu, K. Tang, M. Ke, Z. Liu, Extraordinary acoustic shielding by a monolayer of periodical polymethyl methacrylate cylinders immersed in water, *J. Appl. Phys.* 110 (1) (2011) 014509, <http://dx.doi.org/10.1063/1.3601746>, http://jap.aip.org/resource/1/japiau/v110/i1/p014509_s1.
- [20] H. Estrada, J.M. Bravo, F. Meseguer, High sound screening in low impedance slit arrays, *New J. Phys.* 13 (4) (2011) 043009, <http://dx.doi.org/10.1088/1367-2630/13/4/043009>, <http://iopscience.iop.org/1367-2630/13/4/043009>.
- [21] C. Qiu, R. Hao, F. Li, S. Xu, Z. Liu, Broadband transmission enhancement of acoustic waves through a hybrid grating, *Appl. Phys. Lett.* 100 (19) (2012) 191908, <http://dx.doi.org/10.1063/1.4714719>, http://apl.aip.org/resource/1/applab/v100/i19/p191908_s1.
- [22] A. Elayouch, M. Addouche, E. Herth, A. Khelif, Experimental evidence of ultrasonic opacity using the coupling of resonant cavities in a phononic membrane, *Appl. Phys. Lett.* 103 (8) (2013) 083504, <http://dx.doi.org/10.1063/1.4819021>, <http://scitation.aip.org/content/aip/journal/apl/103/8/10.1063/1.4819021>.
- [23] Z. Yang, J. Mei, M. Yang, N.H. Chan, P. Sheng, Membrane-type acoustic metamaterial with negative dynamic mass, *Phys. Rev. Lett.* 101 (2008) 204301, <http://dx.doi.org/10.1103/PhysRevLett.101.204301>.
- [24] R.P. Moiseyenko, S. Herbison, N.F. Declercq, V. Laude, Phononic crystal diffraction gratings, *J. Appl. Phys.* 111 (3) (2012) 034907, <http://dx.doi.org/10.1063/1.3682113>.
- [25] R.P. Moiseyenko, J. Liu, N.F. Declercq, V. Laude, Blazed phononic crystal grating, *Appl. Phys. Lett.* 102 (3) (2013) 034108, <http://dx.doi.org/10.1063/1.4789767>.
- [26] L.E. Kinsler, A.R. Frey, A.B. Coppens, J.V. Sanders, *Fundamentals of Acoustics*, Vol. 1, 1999.
- [27] D. Royer, E. Dieulesaint, *Ondes élastiques dans les solides*, Wiley, New York, 1999.